

Lawrence Berkeley National Laboratory

Lawrence Berkeley National Laboratory

Title

DEVELOPMENT OF HIGH TEMPERATURE SCANNING ELECTRON
MICROSCOPY AND APPLICATIONS TO SINTERING STUDIES

Permalink

<https://escholarship.org/uc/item/0mz4q94p>

Author

Wang, D.N.K.

Publication Date

1978-04-01

NOTICE

This report was prepared as an account of work sponsored by the United States Government. Neither the United States nor the United States Department of Energy, nor any of their employees, nor any of their contractors, subcontractors, or their employees, makes any warranty, express or implied, or assumes any legal liability or responsibility for the accuracy, completeness, or usefulness of any information, apparatus, product or process disclosed, or represents that its use would not infringe privately owned rights.

DEVELOPMENT OF HIGH TEMPERATURE SCANNING
ELECTRON MICROSCOPY AND APPLICATIONS TO SINTERING STUDIES

D. N. K. Wang, D. J. Miller and R. M. Fulrath

Materials and Molecular Research Division, Lawrence Berkeley Laboratory
and Department of Materials Science and Mineral Engineering,
University of California, Berkeley, California 94720

ABSTRACT

The densification and microstructural changes of a metallic and/or ceramic powder compact during sintering is a critically important but incompletely understood process. Whether solely in the solid state or in the presence of a liquid phase, mass transport occurs at elevated temperatures to eliminate porosity and reduce the surface energy of the system.

Modifications in a commercial specimen heating stage for the JEOL JSM-U3 scanning electron microscope were made for the purpose of increasing the temperature capability of the device.

The present hot stage design enables continuous observation of materials at temperatures up to 1750°C and magnifications up to 5000x. An elevated temperature run at 1750°C has been made over a 24 hour period without heater failure. Design changes center around the construction of a reliable heating element. A thermal electron suppression grid mounted between the specimen heating stage and the secondary electron detector is a requisite component of the instrument. The suppression grid serves the purpose of repelling low energy thermal electrons emitted by materials at high temperatures which can mask the secondary electron image. A turbomolecular pump incorporated into the vacuum system has reduced the problem of hydrocarbon contamination of the sample surface.

Changes in specimen dimensions, particle shape and pore morphology, formation of liquid phases and other direct evidence of the sintering process have been observed and recorded at temperature using video tape and 16mm time lapse movies of the TV scanning image. Materials that have been examined at elevated temperature are Ni, glass, Al_2O_3 , UO_2 , W, Cu, WC-Co, and CaF_2 .

Introduction

Metals and ceramic materials are often subjected to high temperature in processing to activate mass transport. Under the driving force of reducing the surface energy of the system, mass transport occurs at elevated temperatures in powder compacts resulting in a reduction of porosity and grain growth. Changes in pore morphology and the shrinkage of powder compacts during this process of sintering have been described by a number of sintering theories.

In 1970, work was begun on the development of an elevated temperature stage for the scanning electron microscope. The primary goal of this work was the development of an instrument capable of longtime operation at high temperature which could be utilized in sintering studies of metallic and ceramic powders.

Original modifications of a commercial specimen heating device for the JSM-U3 supplied by JEOL have been previously described.¹ These design changes centered around the construction of a more reliable heater, increased radiation shielding and modification of the thermal electron suppression grid. With these initial modifications, the temperature capability of the heating stage was increased from 1100°C to 1600°C. Operation at high temperatures was possible for periods up to five hours.

Continued improvements in the specimen heating stage have enabled the direct observation of materials at temperatures of 1750°C over a 24 hour period.

The purpose of this paper is to specifically describe the improved heating stage design and to present the experimental method and capabilities of high temperature scanning electron microscopy when applied to the study of sintering.

Development of Hot Stage

Heater Design

A nominal 0.265 in. I.D. by 0.405 in. O.D. Lucalox tube was diamond ground to an O.D. of 0.388 in. This tube was threaded by diamond grinding to give 0.025 in. deep V grooves with 26 threads per inch. The tube was cut to give sections 0.35 in. in length. A second tube with nominal dimensions of 0.415 in. I.D. by 0.5 in. O.D. was cut to 0.35 in. in length. At appropriate positions a slot and notches 0.10 in. wide were cut in the tube wall. The smaller tube was mounted on a post and wound with six turns of 0.015 in. thoriated tungsten wire as shown in Fig. 1A. The tungsten wire was then bent and the larger tube slipped over the assembly to hold the tungsten wire in position during high temperature operation. Fine Lucalox insulating tubes were slipped over the tungsten wire. The completed heater assembly is shown in Fig. 1B. Six molybdenum radiation shields were made of 0.003 in. foil with diameters ranging from 0.6 in. to 0.75 in. After cutting V- notches in the shields, they were slipped over the heater wires as shown in Fig. 1C.

Specimen Stage Assembly

Figure 2 shows the assembled specimen stage. The base block is made

of stainless steel. On both sides of the stage and at one end, 99.8% Al_2O_3 plates are used to isolate the electrical connections for the heater and thermocouple from the metal frame. Copper pieces attached to the alumina sideplates pinch around the tungsten heater wire to provide electrical contact points. Six dimpled molybdenum foil disks 0.75 in. in diameter placed under the heater provide bottom radiation shielding. Within the heating element can be seen a molybdenum stand which supports the sample cup. A 5 mil W-5%Re/W-26%Re thermocouple protected by a Lucalox tube was spot welded to a tungsten foil which had been welded to the bottom of this molybdenum stand. The thermocouple wire is looped around screws on the insulating alumina end plate. Electrical connections for the thermocouple and heater are made when the specimen stage is inserted into the main stage. Dimpled molybdenum foil disks with holes of 1/3 in. diameter were used as top radiation shields. The top cover shield was made of niobium and was held in position by screws at the corners of the metal frame. The completed specimen heating stage is seen in Fig. 3.

Main Stage

Figure 4 shows the positioning of the electrical junctions, specimen heater stage and the thermal electron suppression grid of the original commercial design within the main stage. The wires which form the thermocouple connections are 20 mil. W-5%Re/W-26%Re to place the cold junction as far from the heater stage as possible. The specimen stage assembly rests on a water cooled platform which dissipates the heat. The chromium plated shutter above the specimen stage is used for alignment of the primary beam. In long time runs it is also used to shield the pole piece

and aperture from radiation from the heated stage.

Hot Stage Operation

Column Pressure and Specimen Contamination. The original vacuum system consisted of an oil diffusion pump backed by a rotary mechanical pump. Back diffusion of diffusion pump oil and subsequent cracking of hydrocarbons on the irradiated specimen surface resulted in contamination which reduced resolution. Such contamination could also affect mass transport at elevated temperatures. Replacing the oil diffusion pump with a turbomolecular oil-free pump has nearly eliminated the problem of surface contamination. The normal operating pressure in the column of the microscope is approximately 2×10^{-5} torr.

Temperature Measurement and Calibration. Two power sources are used for heating the stage. A constant current D.C. power supply is used for manual operation. Temperature drifts of approximately 20°C per hour have been observed when the temperature is above 1600°C. By manual adjustment a constant temperature is easily maintained.

A variable voltage D.C. power supply driven by an automatic recorder-controller is used for long time runs or when controlled heating rates are desired. Samples of metallic or ceramic powders can be heated to 1700°C in about 10 minutes.

Since the thermocouple wire is not positioned near enough to the specimen being heated, the thermocouple temperature is calibrated to give the true specimen temperature. The set up shown in Fig. 5 is used to accomplish this purpose. The stage is placed in a vacuum chamber that has the same environment as the column of the microscope except for the absence of the electron beam. A calibrated optical pyrometer is focused

on the sample surface viewed through the holes in the top radiation shields. For each pyrometer reading, the thermocouple temperature and the power input to the heating element are recorded. Figure 6 shows the heater power input thermocouple temperature relationship for four rates of heating. Approximately 80 watts are required to heat the specimen to 1700°C and this power is independent of heating rate.

The temperature calibration curves as a function of heating rate are shown in Fig. 7. The specimen temperature is always higher than the thermocouple temperature and the temperature difference changes with changing temperature. For example, at thermocouple temperatures of 1200°C and 1690°C, the specimen temperatures were 1230°C and 1660°C, respectively. The greater deviation of higher temperatures is a result, perhaps, of the increased efficiency of radiant heating. The deviation of the 13°C/min heating curve from those of lower heating rates is thought to be caused by thermal non-equilibrium of the specimen when heated at this fast rate. The temperature calibration curves were supported by observable melting of a variety of metals within the scanning electron microscope.

Applications to Sintering Studies

The sintering kinetics of ceramic and/or metal powder materials are commonly obtained by experimental methods such as dilatometry which provide a measurement of shrinkage of a particle compact as pore volume is reduced at elevated temperatures. Shrinkage or density measurements as a function of time and temperature are predicted by various sintering theories and are analyzed in an effort to establish densification mechanisms.

The features of reliability of high temperature operation to 1750°C and facility of changing magnifications from 50 to 5000x, which the high temperature SEM affords, has provided a new experimental approach to the study of sintering. Successful application of this instrument to the studies of both solid state^{2,3,4} and liquid phase^{5,6} sintering have been made.

Samples for sintering studies are easily prepared by placing loose powders or powders pressed to specific green densities in a sample cup which is then set within the heating element of the specimen carrier. Conductive coatings are not applied to the samples. Prefiring of samples outside the scanning electron microscope is sometimes performed to remove organic binders or to reduce oxide surface layers on metals. Molybdenum, platinum, graphite and alumina sample cups have been used for high temperature SEM experiments. The desire for sample and sample cup to be non-reactive determines which sample cup is chosen.

Where shrinkage kinetics of a powder compact are sought, alumina or tungsten microspheres are scattered on the surface to serve as reference points for shrinkage measurements.

Because changes in the sample's character can occur rapidly at high temperatures, the TV scanning mode is normally used to observe the sintering process. An accelerating voltage of 35 kV and beam currents of 1.0 to 3.0×10^{-8} amps have given the best results. Recording of the TV scan image has been made by video tape, 16mm time lapse movies or by a 35mm still camera.

Samples are heated within the vacuum environment of the SEM using either constant heating rate or isothermal techniques. The resolution

of the sample is dependent upon the material being studied and the temperature of observation. At low temperatures, charging of insulating materials results in very poor resolution. As the sample is heated resolution is improved. The temperature where this improvement occurs is dependent upon the specimen. For silicate glasses this temperature is about 300°C while for alumina it is approximately 800°C. Thermal electron emission from materials begins to have a significantly deleterious effect when the temperature has reached approximately 1100°C. A negative voltage applied to the copper suppression grid is then necessary to repel the low energy thermal electrons which mask the secondary electron emission. A voltage of approximately 5 volts is required at 1750°C to observe alumina or tungsten microspheres.

During heat treatment, a low magnification (~100x) image of the surface of a particle compact is continuously monitored. From time lapse movies of this TV scanning image, the change in dimensions between reference microspheres is measured and the shrinkage and densification are calculated. Using this technique a number of shrinkage measurements are possible at any one temperature and a statistical value of shrinkage is made.

The ease in changing magnification enables monitoring of shrinkage and high magnification observation of geometric changes of pore and particle shape as densification occurs. The ability to clearly view these geometric changes during sintering is typically limited to materials of size greater than one micron. The decrease in resolution caused by specimen stage design, thermal electron emission, charging and possible volatility of some materials in the vacuum environment is the cause for

this limitation.

The use of high magnifications (up to 5000x) in observing liquid phase formation, rearrangement, wetting and solution-precipitation processes make high temperature scanning electron microscopy an especially valuable tool in studying liquid phase sintering.

A variety of ceramic and metallic materials have been observed using the high temperature SEM. Solid state densification kinetics of Ni^2 , UO_2^3 and Al_2O_3 have been studied using the described techniques. The liquid phase densification of WC-Co and Fe-Cu composites was directly observed and the results reported.^{5,6} Microspheres of glass, W, Cu, and CaF_2 have also been observed sintering at elevated temperatures.

Summary

In this paper, the present high temperature stage for the scanning electron microscope has been described. This stage is capable of maintaining temperatures up to 1750°C for long periods of time. The longest run made to date at 1750°C was for a period of 24 hours.

The ability to directly observe ceramic and metallic materials at high temperatures and high magnifications makes the high temperature SEM a uniquely valuable tool for studying solid state and liquid phase sintering. The advantages of this technique include: 1) direct observation of changes in particle and pore shape, liquid phase formation, particle rearrangement and other geometric changes which can occur very rapidly during densification and 2) the ability to obtain statistical shrinkage measurements of a particle compact by a method which will not influence the observed values.

The major problem encountered in high temperature scanning electron microscopy is in high resolution of materials under conditions where charging, thermionic emission of electrons and volatility in the vacuum environment may affect secondary electron detection.

Acknowledgment

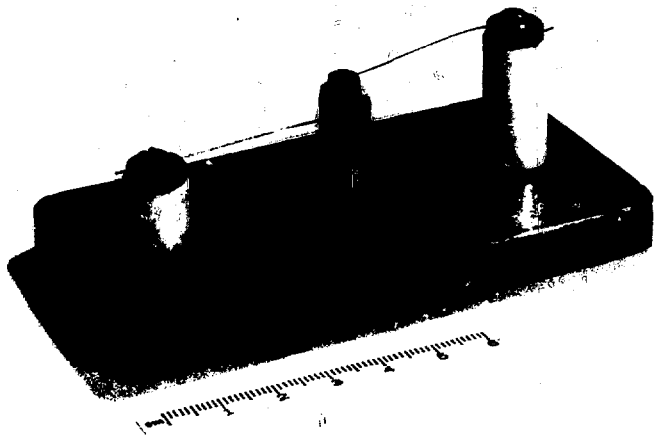
This work was supported by the Division of Materials Sciences, Office of Basic Energy Sciences, U.S. Department of Energy. Thanks are extended to Joseph A. Pask for his suggestions and review of the manuscript.

References

1. R. M. Fulrath, "Scanning Electron Microscopy to 1600°C," in Scanning Electron Microscopy, IIT Research Institute, Chicago, 17-20, 1972.
2. C. B. Shumaker and R. M. Fulrath, "Initial Stages of Sintering of Copper and Nickel," Materials Science Research Vol. 6, Sintering and Related Phenomena. 191-199, Plenum Press, NY, 1973.
3. D. J. Miller, "SEM Hot-Stage Sintering of UO_2 ," M.S. Thesis, LBL-5173, University of California, Berkeley, California, June 1976.
4. D. N. K. Wang, "Sintering of Al_2O_3 Powder Compact by Hot Stage Scanning Electron Microscopy," Ph.D. Thesis, LBL-5763, University of California, Berkeley, California, December 1976.
5. L. Froschauer and R. M. Fulrath, "Direct Observation of Liquid Phase Sintering in the System Iron-Copper," J. Mat. Sci., 10, 2146-2155, 1975.
6. L. Froschauer and R. M. Fulrath, "Direct Observation of Liquid Phase Sintering in the System Tungsten Carbide-Cobalt," J. Mat. Sci., 11, 142-149, 176.

Figures

- Fig. 1. Construction of heating element (A) tungsten wire wound on Lucalox tube (B) completed heating element (C) heating element surrounded by molybdenum radiation shields.
- Fig. 2. Specimen stage carrier (A) alumina side plate (B) molybdenum stand within heating element (C) top moly radiation shields (D) niobium cover plate.
- Fig. 3. Fully assembled high temperature stage (A) copper heater connection (B) W-5%Re/W-26%Re thermocouple wire.
- Fig. 4. Detail of main stage (A) copper heater electrical connections (B) W-5%Re/W-26%Re thermocouple junction (C) water cooled base plate (D) specimen heater stage in position (E) thermal suppression grid (F) chromium plated shutter.
- Fig. 5. Experimental arrangement for thermocouple calibration (A) optical pyrometer (B) main stage (C) diffusion and mechanical vacuum pump (D) power supply and automatic recorder controller.
- Fig. 6. Heater power input versus thermocouple temperature as a function of constant heating rate.
- Fig. 7. Specimen temperature from optical pyrometer versus thermocouple temperature as a function of heating rate.



A

XBB782-1426

Fig. 1 (A).



B

XBB782-1424

Fig. 1 (B).

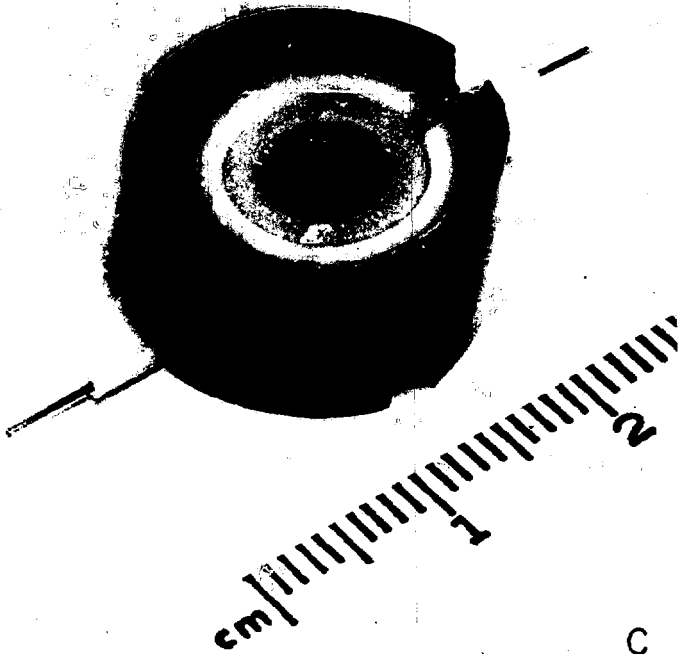


Fig. 1 (C)

XBB782-1423

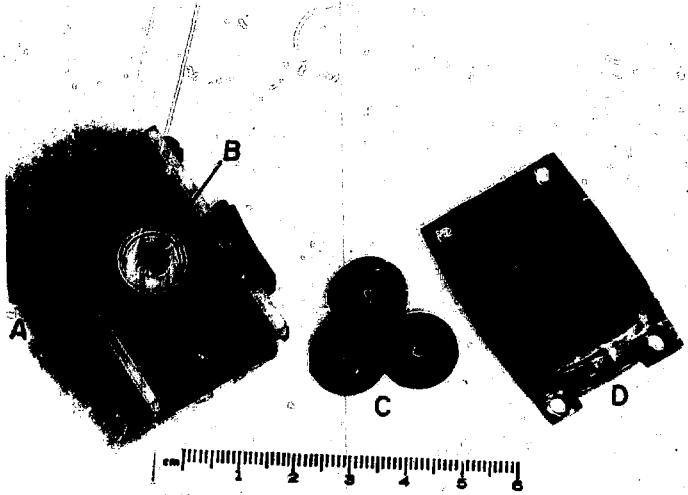


Fig. 2

XBB782-1425

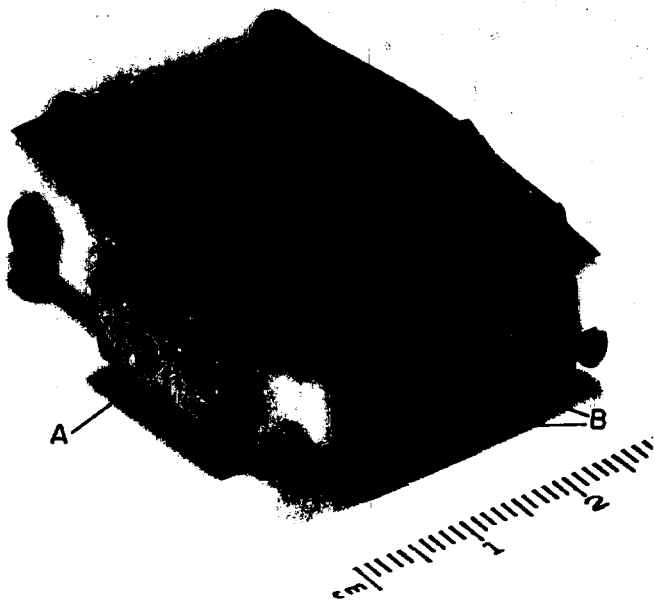


Fig. 3.

XBB782-1422

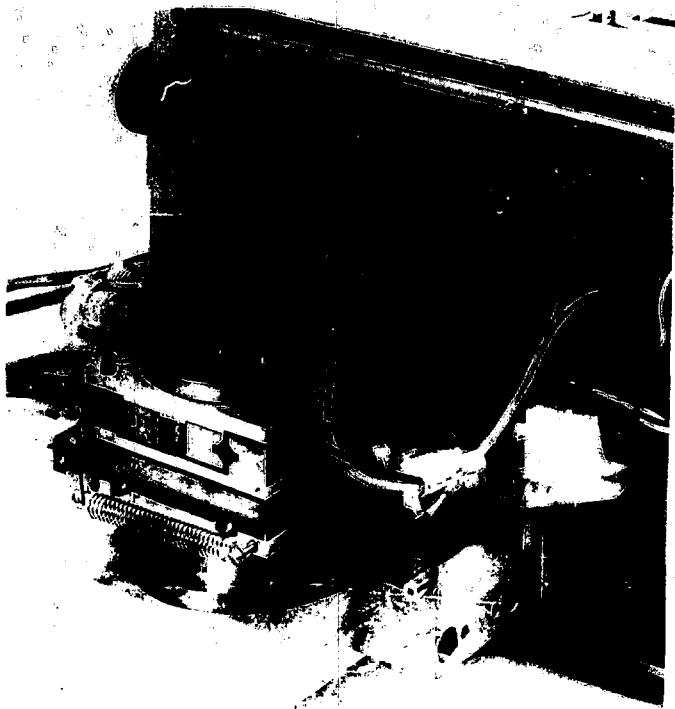


Fig. 4 (A)(B)

XBB782-1419

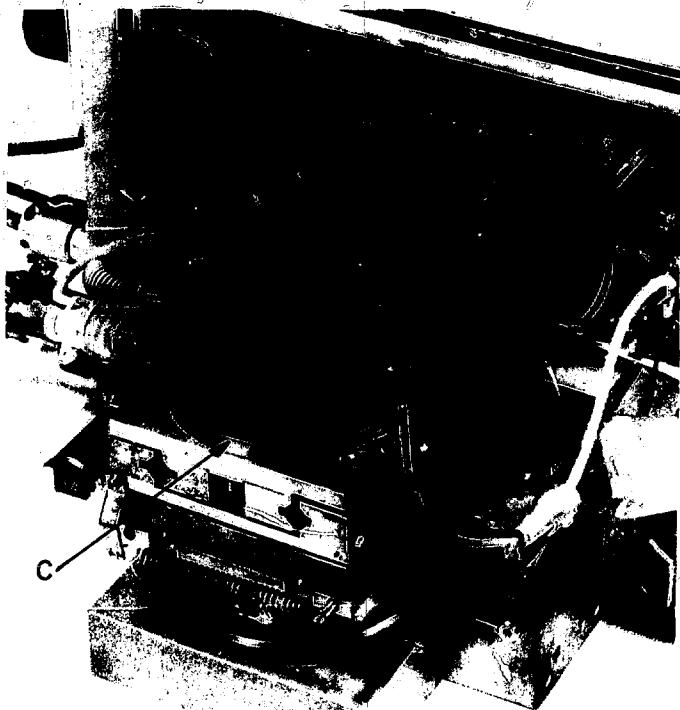


Fig. 4 (C)(D)

XBB782-1420



Fig. 4 (E) (F)

XBB-782-1421

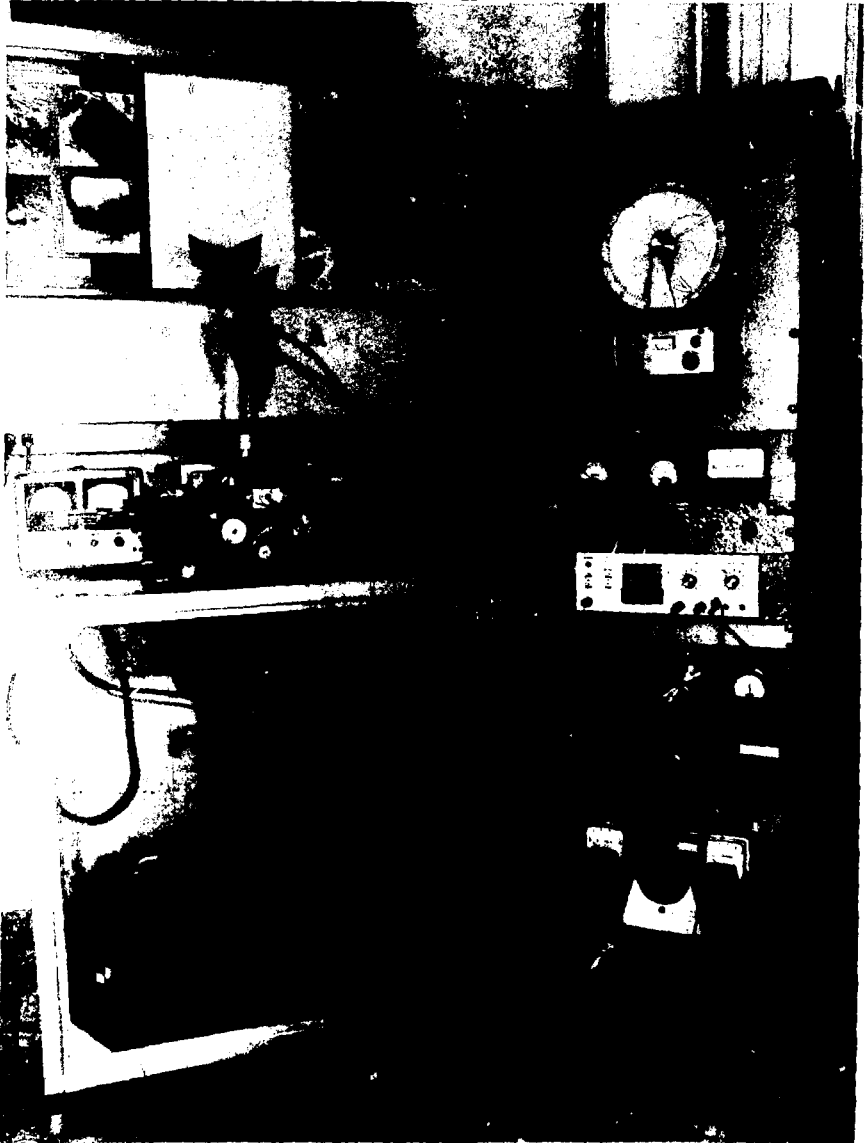


FIG. 5

XBB763-2421

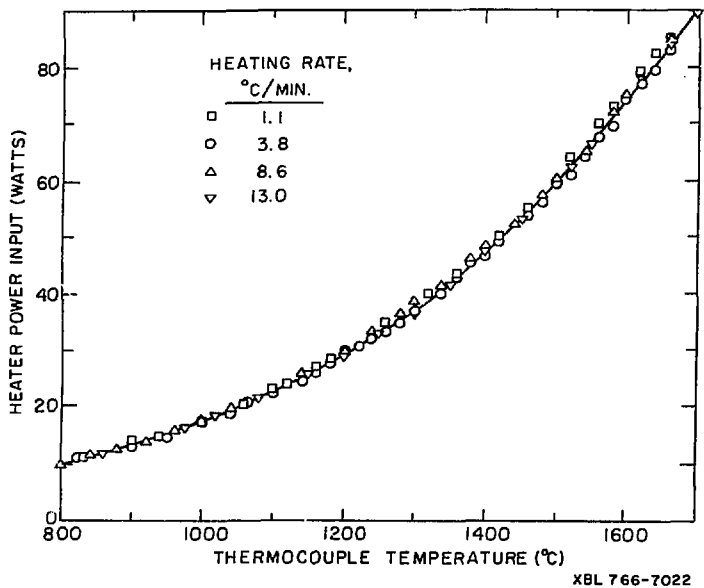
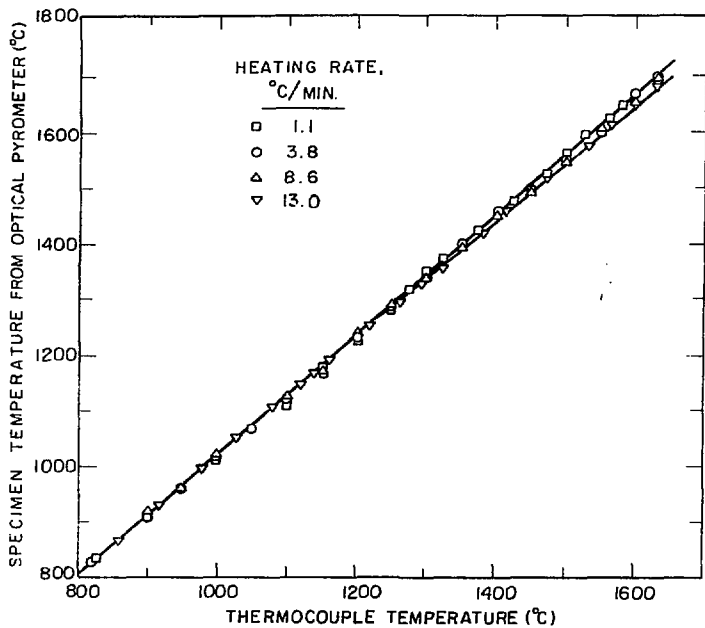


Fig. 6



XBL 766-7023

Fig. 7